JOURNAL OF PROPULSION AND POWER
Vol. 27, No. 1, January–February 2011

Theoretical and Experimental Identification of Acoustic Spinning Mode in a Cylindrical Combustor

Mark Sliphorst,* Stefan Gröning,† and Michael Oschwald‡
DLR, German Aerospace Center, Lampoldshausen, 74239 Hardthausen, Germany

DOI: 10.2514/1.49230

The analytical solution for the eigenmodes of a cylindrical combustor allows for several realizations of the first tangential mode. The limiting cases of standing and spinning first tangential modes are well known. The general solution for a first tangential mode, however, allows for a large variety of realizations. In this study the analytical solution of the acoustic problem and a numerical time-resolved simulation of the acoustic pressure field are compared with experimental data from hot-fire tests. The experimentally observed pressure data are in excellent agreement with the simulation for all possible theoretical solutions. The approach enables detailed insight into the dynamics of the pressure field and thus constitutes a tool for the characterization of acoustic pressure waves in a cylindrical combustor even when the amplitude of the investigated eigenmode is small as compared with the mean pressure fluctuation.

Nomenclature

A	=	amplitude
a	=	speed of sound, m/s
D_t	=	nozzle throat diameter, mm
J	=	fuel-to-oxidizer momentum-flux ratio
J_n	=	Bessel function of order, n
L	=	length of combustor
l	=	order of longitudinal mode
M	=	amplitude of clockwise spinning mode
m	=	order of radial mode
$\dot{m}$	=	mass-flow rate, g/s
N	=	amplitude of counter-clockwise spinning mode
n	=	order of tangential mode
p	=	pressure, Pa
$\dot{q}$	=	heat release, W/s/m^3
R	=	radius of combustor, m
ROF	=	oxidizer-to-fuel mass-flow ratio
r	=	radius, m
T	=	temperature, K
t	=	time, s
v	=	injection velocity, m/s
We	=	Weber number
z	=	length, m
$\alpha_{n,m}$	=	abscissa of $(m+1)$th extremum of Bessel function of order n
δ	=	mode orientation for $t = 0$ rad
θ	=	angle, rad
φ	=	orientation of nodal line, rad
ω	=	angular frequency, rad/s

Subscripts

$()_l$	=	order of longitudinal mode
$()_m$	=	order of radial mode
$()_n$	=	order of tangential mode

Superscript

$()'$	=	fluctuating part

Introduction

HIGH-FREQUENCY combustion instabilities have been an issue troubling rocket combustion chamber developers ever since the beginning of space transportation. Although a lot of experience has been obtained [1,2] and basic mechanisms for the coupling of combustion and acoustics have been identified the search for a fundamental approach to prevent high-frequency combustion instabilities in general has been unsuccessful. Strategies and solutions to avoid combustion instabilities are still mainly based on empirical solutions, often stability can only be achieved by passive damping elements like baffles or absorbers. Detailed experimental investigation of the combustion process at representative conditions is a difficult task even for steady state operation and even more challenging for an unstable system where a high temporal resolution is required. Thus combustion instabilities are still considered one of the most complicated and badly understood problems in rocket combustion chambers. Because of the hazardous effects instabilities have on rocket engine performance, or even the destructive effect on the engine itself, they are also considered one of the most dangerous.

The effect of an acoustic wave with a pressure amplitude p' in a rocket combustor on combustion processes like injection, atomization, droplet atomization, etc., can result in a modulation of the heat release $\dot{q}'$. For specific conditions this results in energy transfer from the combustion process into the acoustic wave resulting in a combustion instability. Rayleigh [3] was the first to postulate in 1878 that to excite an acoustic instability, heat must be added to a gas at the moment of greatest compression, and subtracted at the moment of deepest depression. This was later captured mathematically in the following more general form, known as the Rayleigh criterion:

$$\int_V \int_0^T p' \dot{q}' \, \mathrm{d}t \, \mathrm{d}V > 0 \tag{1}$$

Equation (1) gives a necessary condition for a positive feed back of acoustics and combustion: the integral can only have a positive value if the phase shift between pressure fluctuation and heat release is less than ± 90 deg. A more thorough discussion can be found in Putnam [4] or Yang and Anderson [2].

To be able to calculate the integral of Eq. (1) and determine whether a positive coupling between acoustics (pressure fluctuation) and combustion (heat release) takes place, one must first identify the dynamic pressure field. The present study is thus addressing the

Received 5 February 2010; revision received 19 August 2010; accepted for publication 30 August 2010.

*Ph.D. Student.
†Master's Student.
‡Head of Rocket Propulsion.

experimental identification of tangential modes in a research combustion chamber. First, the general solution for the 1T acoustic mode in a cylindrical resonator is discussed. It will be shown that the solutions are more complex than the usually discussed standing or spinning modes. Then experimental data of dynamic pressure measurements in our experimental combustor are analyzed. It is shown that all predicted possible realizations of the spatial and temporal evolution of the first tangential (1T) mode are found in the experiment and that the data allow a detailed reconstruction of the temporal evolution of the acoustic mode.

Experimental Setup

Combustion Chamber

All experiments were executed in the common research chamber (CRC) model combustor with the propellant combination liquid oxygen (LOX) and gaseous methane (CH_4). The cross section of the CRC is shown in Fig. 1. Knapp et al. [5] give a more thorough description of the CRC. This combustor was specifically designed for combustion instabilities research. The CRC has a diameter of 200 mm, and a length of only 40 mm. These dimensions were picked such that the longitudinal eigenmodes would not be in the same order of magnitude as the transversal modes and therefore not interfere with the measurements thereof. Also, due to this geometry, the frequencies of the tangential modes during hot-fire experiments are representative for full scale engines. An overview of some fundamental eigenfrequencies of the CRC is presented in Table 1.

The CRC has 16 modules in its wall, which can be equipped with sensory equipment, or other hardware for specific research. The coaxial injector is always built in module 1 which is equipped with cooling channels and is cooled with liquid nitrogen to guarantee oxygen to remain liquid in the injector for the duration of a test. The main nozzle is mounted in axial direction. In respect to the disk like combustor volume and the radial injection of the propellants, the concept of the setup is similar to that used by Heidmann [6].

Hot-Fire Tests

The hot flow tests were performed with LOX and CH_4. The propellants are injected with a single element shear coaxial injector in radial direction. The LOX post is tapered (full angle 13 deg) but has no recess. The internal and external diameters of the LOX post at injector exit are 2.5 mm and 3.15 mm, respectively. The diameter of the CH_4-annulus is 5 mm. Experiments were executed fuel rich, with an equivalence ratio range of 0.5 to 1.0. Fuel mass-flow rate was varied from 0.88 to 5.6 g/s, and the range of oxidizer mass-flow rate was between 3.1 to 15 g/s. Hot-fire tests have a duration of 10 seconds after ignition, where it is assumed that the transient phase is terminated, and thus stationary combustion takes place, 3 seconds after ignition. Main nozzles with different diameters are available. With the different mass-flow rates, a range of between 2 and 10 bar can be achieved for the chamber pressure. The chamber was equipped with 6 dynamic pressure sensors (Kistler, Type 6125), mounted in the modules 4, 5, 6, 8, 10, and 15. The sampling rate of these sensors was 32 kHz.

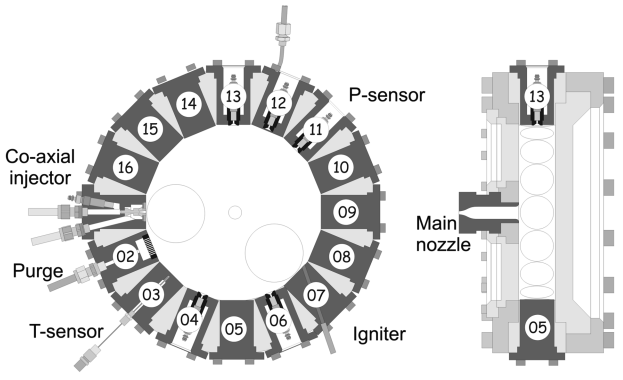

Fig. 1 Cross section of the CRC.

Table 1 Eigenfrequencies in CRC

Mode	Frequency
1T	2490 Hz
2T	4131 Hz
1R	5185 Hz
1L	10625 Hz

Table 2 Operating conditions

Parameter	Value
p_C	9.3 bar
$\dot{m}_{\text{total}}$	9.0 g/s
ROF	3.5
D_t	5.0 mm
v_{CH4}	25.4 m/s
v_{LOX}	1.2 m/s
J	2.5
We	750
T_{CH4}	260 K
T_{LOX}	80 K

The presented analysis was performed for a large number of operating conditions for which results of similar quality were obtained. Therefore only one operating point is presented in this paper. The conditions of this operating point are given in Table 2. Typical root mean square (rms) values for the dynamic pressure component p'_C for all operating points were about 1%. The acoustic pressure levels thus were below that for which combustion would be classified as unstable [7].

Excitations of the 1T Mode in the CRC

It is usually assumed that the acoustic field takes the form of a standing wave, as for example is discussed in Harrje and Reardon [1] and Yang and Anderson [2]. Spinning waves have also been theorized and discussed in the 1960s by Clayton et al. [8] and 1970s by Harrje and Reardon [1], and more recently by Litchford and Luo [9]. Spinning modes are considered the most violent and dangerous.

Thus when analyzing the dynamic pressure field in the CRC in the frequency range of the 1T mode we had expected to identify either standing waves or spinning waves. A standing wave on the circumference of the combustor wall p', as it will be shown in the next section, should show the following behavior:

$$p'(\theta, t) = A\cos(\theta)\cos(\omega t) \tag{2}$$

The temporal variation of p' measured by the sensors should be in phase for all angular positions. The amplitude should vary along the tangential position θ with zero amplitude for $\theta = 90$ and 270 deg, according to the nodal line of the standing wave.

For a spinning mode the dependence of p' on θ can be described as follows:

$$p'(\theta, t) = A\cos(\theta + \omega t) \tag{3}$$

For the spinning wave at any instant in time there is an angle θ for which $\cos(\theta + \omega t) = 1$ and thus p' is maximum. The location of this maximum will rotate along the circumference of the combustor wall. Hence, the dynamic pressure sensors should detect signals of the same amplitude, but with a phase shift corresponding to their mounting position.

Summarizing, if a standing wave presents itself in the CRC, the signals measured by sensors distributed around the circumference of the combustor must be either in phase or in antiphase because the nodal line is at a fixed position. For a spinning wave the amplitudes must all be constant, with varying phases between the sensors. In Fig. 2 an exemplary sample of wall pressure measurements recorded in the CRC shows that the signals from different sensors are not in phase and the amplitudes are not equal. Thus the measured data did

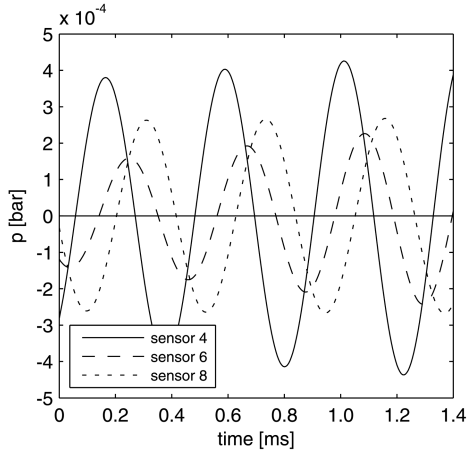

Fig. 2 Sample of wall pressure measurements.

neither match the signature neither of a standing nor that of a spinning mode. Furthermore the characteristics of the signals has been observed to vary with time.

The present study therefore starts with an analysis of the solution of the acoustic wave equation for a resonator with cylindrical symmetry and then reevaluates the experimentally obtained acoustic pressure fields in the CRC.

Spinning Modes

General Description

The acoustic pressure field for an arbitrary volume is generally described by the following three-dimensional wave equation, which can be found in any gas dynamics text book, for example Zucrow and Hoffman [10]:

$$\frac{\partial^2 p'}{\partial t^2} - a^2 \Delta p' = 0 \tag{4}$$

This is a linear, hyperbolic partial differential equation.

Because the CRC is a circular cylinder, it is possible to analytically solve this equation for the given geometry. If Eq. (4) is expressed in polar coordinates and the following ansatz,

$$p'(r, \theta, z, t) = R(r)\Theta(\theta)Z(z)T(t)$$

one finds through separation of variables a system of four ordinary differential equations, which can all be solved individually. The following boundary conditions are applied:

1) At any cylinder wall, the velocity in normal direction to the wall is zero.

2) The function must be finite for all values of r, θ, z and t.

3) The solution must be periodic in θ with a period of 2π.

This will yield the general solution for the acoustic pressure field in the CRC. The general solution is

$$p'(r, \theta, z, t) = \sum_{l,m,n} J_n\left(\alpha_{nm}\frac{r}{R}\right)\cos\left(l\pi\frac{z}{L}\right)\cdot(A\cos(n\theta)\cos(\omega t) + B\cos(n\theta)\sin(\omega t) + C\sin(n\theta)\cos(\omega t) + D\sin(n\theta)\sin(\omega t)) \tag{5}$$

Applying trigonometric identities this can be written in a more convenient form:

$$p'(r, \theta, z, t) = \sum_{l,m,n} J_n\left(\alpha_{nm}\frac{r}{R}\right)\cos\left(l\pi\frac{z}{L}\right)\cdot(M\cos(n\theta + \omega t - \delta_1) + N\cos(n\theta - \omega t - \delta_2)) \tag{6}$$

Obviously, this solution consists of three parts:

1) The longitudinal mode is described by $\cos(l\pi z/L)$.

2) The radial mode is described by the Bessel function J_n and its dependence on r/R.

3) The tangential mode is described by two propagating waves that move in opposite direction, with arbitrary constant amplitudes M and N.

The constant phase angles δ_1 and δ_2 define the orientation of the mode at time $t = 0$, and can be chosen freely. They will be set to zero in the further discussion. The integers l, m, n denote the mode numbers.

Limiting Cases of the Spinning 1T Mode

In this study, the focus lies on the 1T mode, i.e., $m = l = 0$ and $n = 1$. This yields for the acoustic pressure field of the 1T mode

$$p'(r, \theta, t) = J_1\left(\alpha_{10}\frac{r}{R}\right)\cdot(M\cos(\theta + \omega t) + N\cos(\theta - \omega t)) \tag{7}$$

Using trigonometric identities it can be seen that if $M = N$ the two propagating waves through superposition result in a standing wave:

$$p'(r, \theta, t) = 2MJ_1\left(\alpha_{10}\frac{r}{R}\right)\cos(\theta)\cos(\omega t) \tag{8}$$

As seen in Eq. (8) the pressure field has the same phase at all tangential positions θ. For the CRC the pressure signals will thus be either in phase or in antiphase, as is illustrated in Fig. 3.

If in Eq. (7) either M or N is equal to 0, only one propagating wave remains. So, assuming $N = 0$, this results in a clockwise propagating wave and the acoustic pressure field is described by Eq. (9):

$$p'(r, \theta, t) = MJ_1\left(\alpha_{10}\frac{r}{R}\right)\cos(\theta + \omega t) \tag{9}$$

A synthetic signal for the CRC is shown in Fig. 4. The pressure field is rotating with angular frequency ω, hence the amplitude recorded by all sensors is identical. The phase between the signals is obviously corresponding to the angle between the sensor positions.

General Characteristics of the 1T Mode

Generally, M and N are neither equal to each other, nor equal to 0. Before discussing an experimentally measured acoustic pressure field during a hot-fire test this general case will be discussed analytically. As the sensors in the CRC are mounted on the chamber wall the pressure in Eq. (7) is evaluated for $r = R$:

$$\begin{aligned} p'(\theta, t) &= J_w(M\cos(\theta + \omega t) + N\cos(\theta - \omega t)) \\ &= J_w(2M\cos(\theta)\cos(\omega t) + (N - M)\cos(\theta - \omega t)) \end{aligned} \tag{10}$$

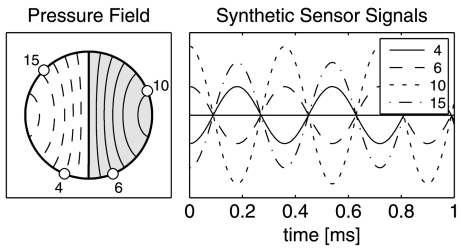

Fig. 3 Acoustic pressure field of standing wave.

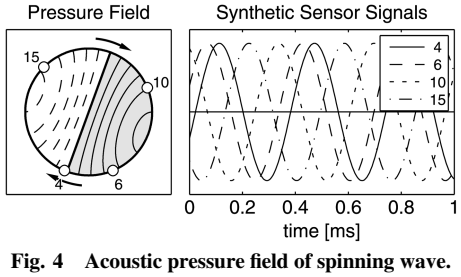

Fig. 4 Acoustic pressure field of spinning wave.

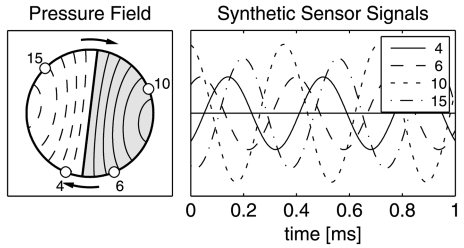

Fig. 5 Acoustic pressure field of propagating wave.

where $J_w = J_1(\alpha_{10})$ has been used, which is the value of the Bessel function on the combustion chamber wall. Obviously the general case of a propagating 1T mode can be seen as the superposition of a standing and a spinning wave. An example of such a general pressure evolution on the combustor wall for arbitrary values of M and N is shown in Fig. 5. Thus the acoustic field recorded by the sensors in the general case of a propagating wave exhibits amplitudes varying with the tangential sensor position and phase differences between the sensor signals not corresponding to their geometric position.

It can be shown analytically that Eq. (10) can be reduced to

$$p'(\theta, t) = A(t)\sin(\theta - \varphi(t)) \tag{11}$$

with

$$A(t) = J_w\sqrt{M^2 + N^2 + 2MN\cos(2\omega t)} \tag{12}$$

By convention the amplitude is defined to be always positive. Using Eq. (12) for the phase φ following dependence on M and N is obtained:

$$\varphi(t) = -\arcsin\left(\frac{\cos(\omega t)\cdot(M+N)}{\sqrt{M^2 + N^2 + 2MN\cos(2\omega t)}}\right) \tag{13}$$

The solutions given for amplitude and phase angle are only valid for $N \geq M$ and in the first half period of an oscillation ($t = 0 - 1/(2f)$). The solutions for $N \leq M$ and any t can be found in the master thesis of *S*. Gröning [11]. The angle φ defines the time dependent orientation of the acoustic pressure field of the 1T mode in the combustion chamber. It can be interpreted as the rotation angle of the nodal line as illustrated in Fig. 6. For the angular velocity with which the nodal line changes its orientation one obtains

$$\dot{\varphi}(t) = -\omega\cdot\frac{(M+N)(M-N)}{(M-N)^2 + 4MN\cos^2(\omega t)} \tag{14}$$

The orientation of the nodal line φ and the rate of change $\dot{\varphi}$ do only depend on the ratio N/M. In Figs. 7 and 8 the temporal development of φ and $\dot{\varphi}$ are shown during a half period. For small values for N/M, which means $M \gg N$, the angle of orientation increases almost linearly, which in turn means that the angular velocity is almost constant, a behavior similar to that of the limiting case of a spinning

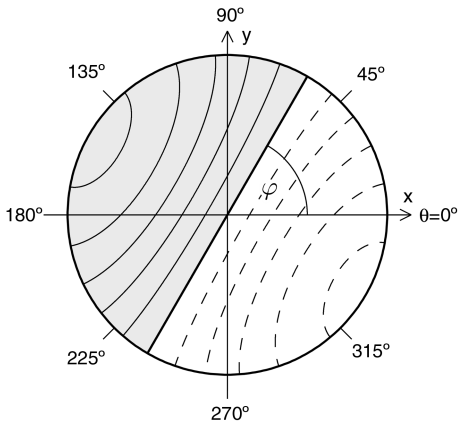

Fig. 6 Interpretation of phase angle as rotation angle.

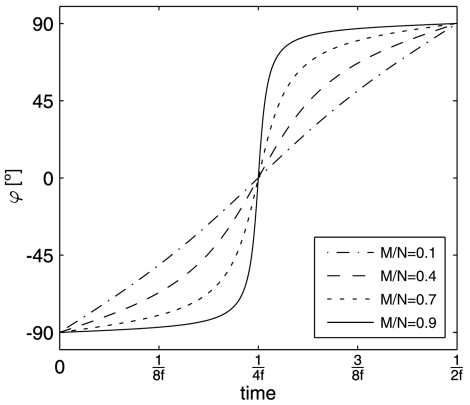

Fig. 7 Development of the orientation of the nodal line of the 1T mode during a half period.

mode. If N/M approaches one, the angle does not change much at all until t approaches $1/(4f)$ as for the limit case of a standing wave. Near to $1/(4f)$ the angle increases very rapidly until its rate of growth decreases again to almost zero after the transition. In the limit $N = M$

$$\varphi = -\frac{\pi}{2}\cdot\mathrm{sgn}(\cos(\omega t)) \tag{15}$$

can be derived. This implies that the orientation of the acoustic pressure field of the standing wave instantaneously jumps from $-\pi/2$ to $\pi/2$ at $t = 1/(4f)$.

Experimental Identification of Propagating Modes

Data Reduction

To be able to investigate the behavior of the eigenmode, it is necessary to extract the relevant information from the experimentally obtained raw pressure signals. The data acquisition rate of 32 kHz is sufficient, respecting the Nyquist sampling-theorem, to resolve the 1T mode with a typical frequency of 2.5 kHz. These raw pressure signals contain all possible acoustic eigenmodes which by superposition contribute to the combustion noise as can be seen in the fast Fourier transform (FFT) spectrum of the dynamic pressure p' in Fig. 9. The resonance frequencies in Fig. 9 show some small deviations from the calculated frequencies in Table 1. This is due to the fact that the speed of sound in the reactive flow in the combustor is spatially dependent.

This FFT spectrum is used to determine the frequency of the 1T mode. Secondly, p' is then band pass filtered around this frequency. To guarantee that the phases of the signals are not influenced by the filtering process a two way filtering procedure is used [12]. A Butterworth band pass filter with the 1T frequency as center frequency is applied on the signal once in forward and once in backward direction. Thus the filtered signal has a zero-phase shift with respect to the unfiltered signal. As could be seen in Fig. 8 the rate of change $\dot{\varphi}(t)$ of the orientation of the nodal line can reach very high

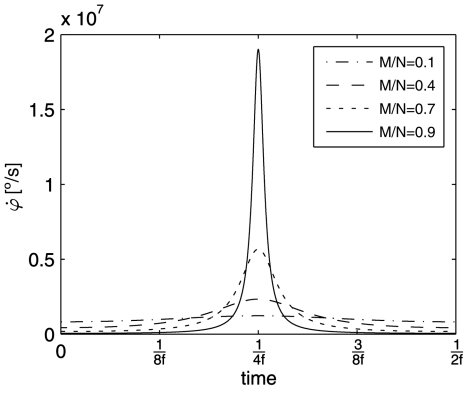

Fig. 8 Development of angular velocity during half period.

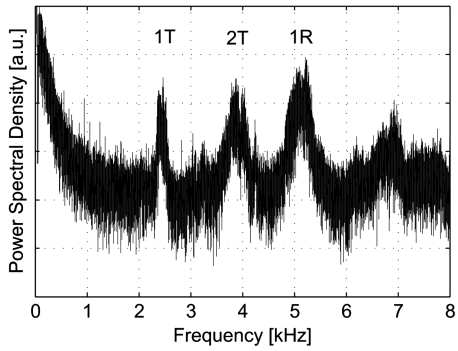

Fig. 9 Power spectral density of pressure sensor raw signal.

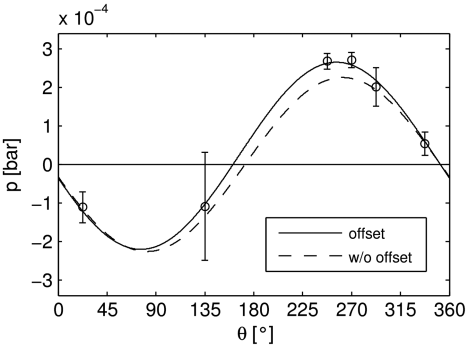

Fig. 11 Fitted sine function to measurements.

values. To enable the required temporal resolution of $\dot{\varphi}$ it was necessary to resample the filtered signals at 200 kHz or even higher during data analysis. In Fig. 10 the filtered and resampled 1T component of the signal is compared with the unfiltered signal.

To estimate the noise level of the recorded signals data have been recorded in the pressurized combustor without flow and combustion, at a pressure level of 10 bar. Although all sensors were of the same type, the rms of the measured noise appeared to be depending on the individual sensor, varying between 0.5 and 3.6 mbar. For the data analysis only the noise in the analyzed frequency range around the 1T mode is relevant and thus the rms values of the filtered signals have been evaluated. The rms values of the filtered noise were between 0.02 and 0.14 mbar and these values are shown in Fig. 11 as error bars. As can be seen the sensor at $\Theta = 135$ deg has a much higher rms value than the other sensors.

Acoustic Pressure Field Determination

The 1T contributions of the dynamic pressure p' for the 6 dynamic pressure sensors provide information on the pressure distribution of the 1T mode at the angular positions where the sensors were mounted. To reconstruct the pressure field on the chamber wall for all tangential angles θ, a pressure distribution $p'(\theta)$ following Eq. (11) is fitted to the experimental data as shown in Fig. 11. The circles are from a sample of dynamic pressures at one specific time instant to which a sine function is fitted. Part of the data show an offset, meaning that the dynamic pressure fluctuation is not symmetric around zero:

$$p'(\theta, t) = A \sin(\theta - \varphi) + p'_{\text{off}} \tag{16}$$

The value of p'_{off} as determined from the experimental data is small and the reason for this offset is not quite understood as today. The fitting procedure has been performed with and without p'_{off}, and the results obtained for the essential characteristics of the 1T mode are practically identical. Figure 11 shows both fits, with and without offset. A very good agreement has been found between experimental data and the prediction by Eq. (16) for all data sets.

The data presented here have been obtained with the offset term included as the fits result in a smaller residual. To minimize the error of the fit procedure, a least squares method with a trust-region algorithm [13] is used. The orientation of the nodal line $\varphi(t)$ for the duration of one test is shown in Fig. 12. Although the direction of the movement of the nodal line is seen to change frequently, a preferred direction for the rotation of the nodal line is found in this test. The

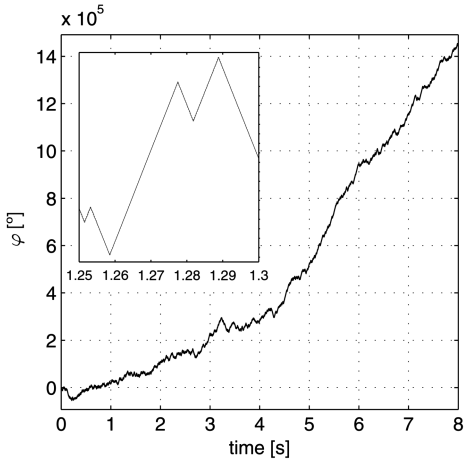

Fig. 12 Development of the orientation of the 1T mode during one test.

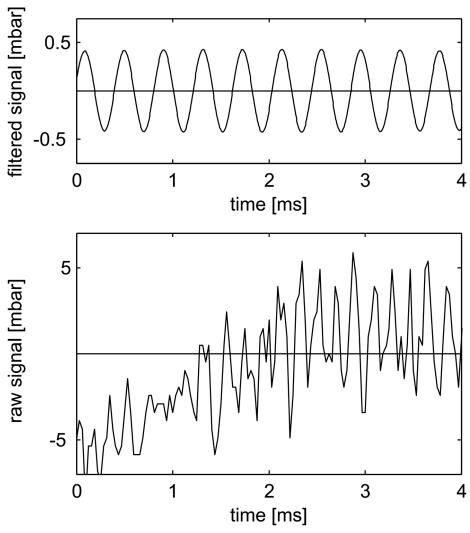

Fig. 10 Raw data of the dynamic pressure and filtered 1T signal.

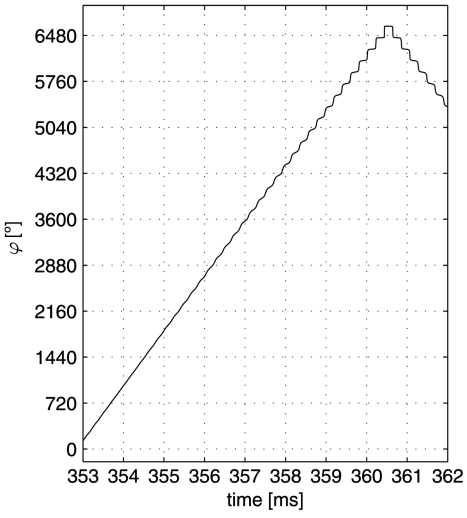

Fig. 13 Zoom into the mode orientation during a direction change.

insert shows a zoom into 50 ms of test duration and a typical time scale for the periods between direction changes is about 10 ms, equivalent to 38 oscillations of the 1T mode. A close-up to a time interval where a direction change is found is shown in Fig. 13. The direction change always happens according to the same sequence of events. A spinning wave with a rotating nodal line with constant angular velocity changes its character slowly into a standing wave with fixed nodal line. The angle's rate of change is almost constant first and exhibits an increasing stepwise character, exhibiting all features already seen in Fig. 7 for the various ratios M/N. In the data shown in Fig. 13 an almost rotating wave with constant angular velocity develops into a standing wave in less than 8 ms. The different characters of the rotating wave that occur in the CRC are shown in the image sequences of Figs. 14 and 15. Figure 14 shows a propagating wave with almost constant angular velocity. Note that the samples shown are equidistant and show a constant change of orientation. Figure 15 shows an almost standing wave with a very high rate of change of the orientation angle φ in the middle of the sequence.

To analyze the sensitivity of the algorithm on measurement errors, simulated pressure sensor signals of a spinning mode have been superposed with synthetic white noise. The rms value of the synthetic noise in the 1T frequency range was 0.12 mbar, about the value of the sensor at $\Theta = 135$ deg. This synthetic noise has been applied to the simulated signals of all sensors, thus this can be seen as a worst case simulation. The mean relative error of the calculated signal $A(t)$ in this case has been found to be $\Delta A/A$=13%, while the mean absolute phase error of the nodal line orientation $\Delta\varphi$ is 15 deg.

Determination of M and N, the Spinning Mode's Character

The coefficients M and N for the clockwise and counter-clockwise spinning waves, respectively, can be obtained from the measured

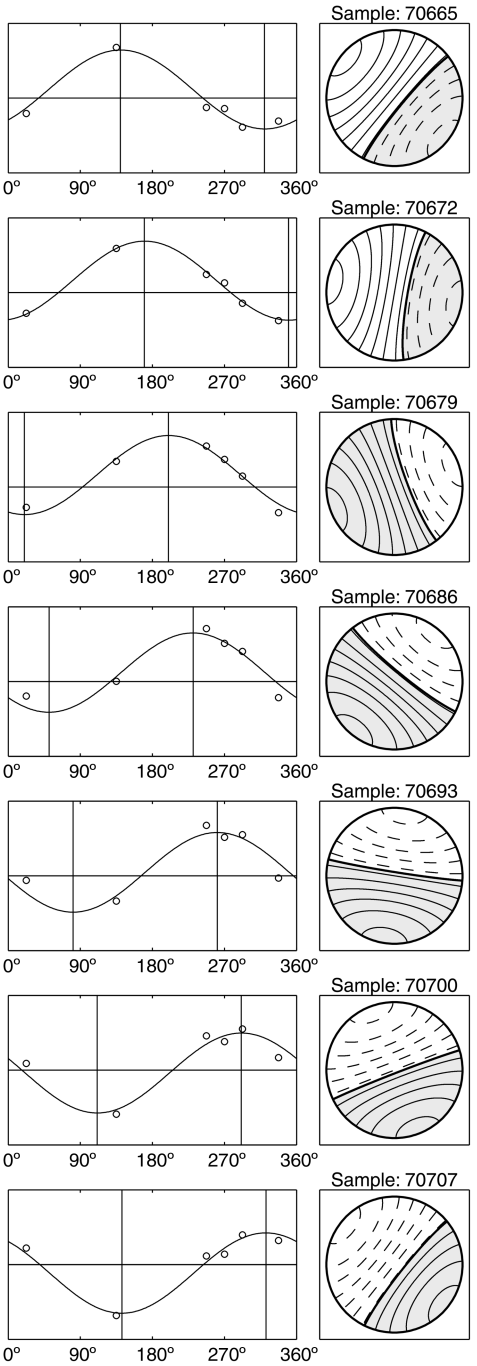

Fig. 14 Sequence of orientations of the 1T mode with rather constant $\varphi(t)$ as typical for a spinning mode.

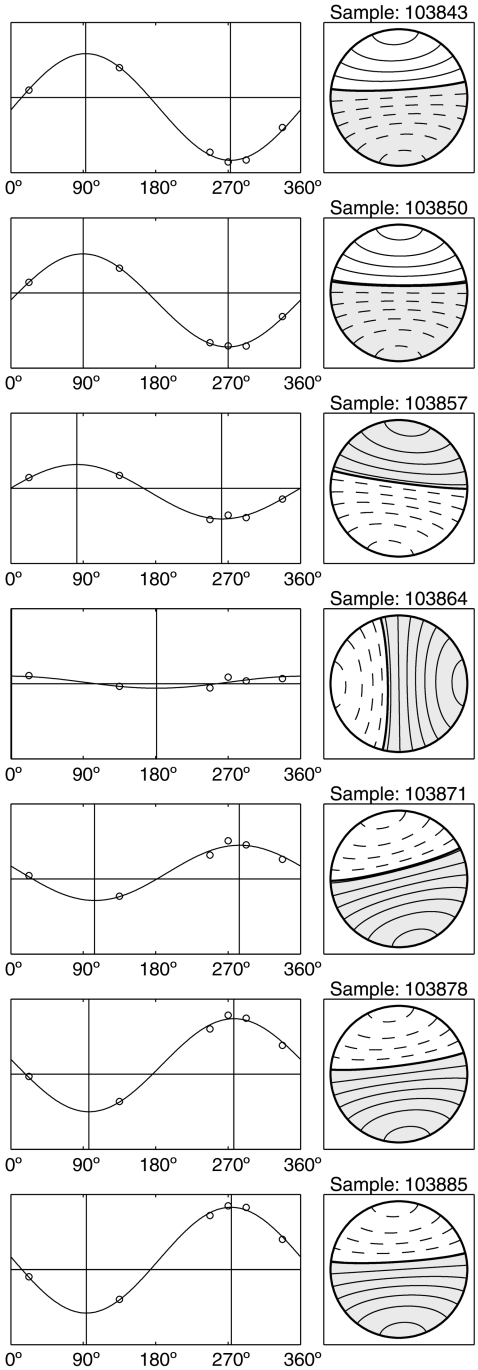

Fig. 15 Sequence of orientations of the 1T mode with rather stepwise variation of $\varphi(t)$ as typical for a standing mode.

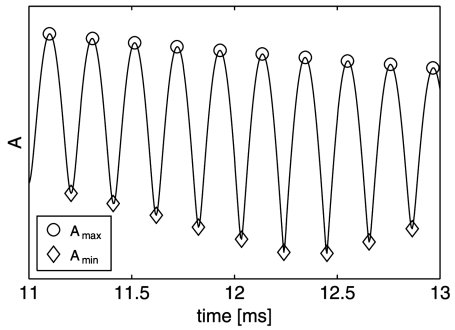

Fig. 16 Development of the amplitude with time.

amplitude $A(t)$ by inversion of Eq. (12). By determining the maximum $A_{\max}$ and minimum $A_{\min}$ of $A(t)$ during one period when $\cos(2\omega t) = \pm 1$ the following equations are obtained:

$$A_{\max} = J_w(M + N) \tag{17}$$

$$A_{\min} = J_w|M - N| \tag{18}$$

where the convention is used that A, M and N are always positive number. Resolved for M and N these relations become

$$M = \frac{A_{\max} + A_{\min}}{2J_w} \tag{19}$$

$$N = \frac{A_{\max} - A_{\min}}{2J_w} \tag{20}$$

The evolution of $A(t)$ as determined from the experimental data is shown in Fig. 16. The values of $A_{\max}$ and $A_{\min}$ used to determine $M(t)$ and $N(t)$ are marked by circles and diamonds, respectively.

The development of M and N during a brief time interval is shown in Fig. 17. For $M > N$, the spinning mode's direction of rotation is clockwise and if $M < N$ it is counter-clockwise. If the two curves intersect, i.e., $M = N$, the acoustic field takes the form of a standing wave. The evolution of the phase φ shows a direction change at the same instant.

Preferred Orientation of the Propagating Wave

The evolution of the propagating waves seems to be a fairly arbitrary process. However the propagating wave apparently has a preferred orientation. For every time instant the orientation φ of the nodal line is evaluated and the data are shown as a histogram in Fig. 18. The orientation has a preferred orientation around $\theta \approx 110$ deg. Indeed the symmetry of the CRC is not perfectly cylindrical. The igniter, the injector, orifices for purge gases, all

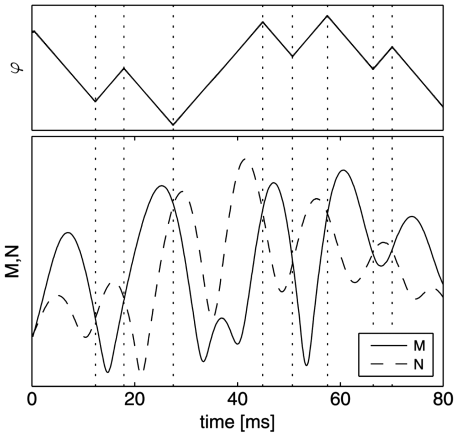

Fig. 17 Development of M, N and phase.

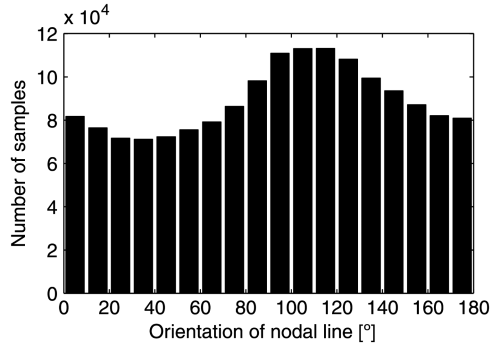

Fig. 18 Probability density of the orientation of the nodal line.

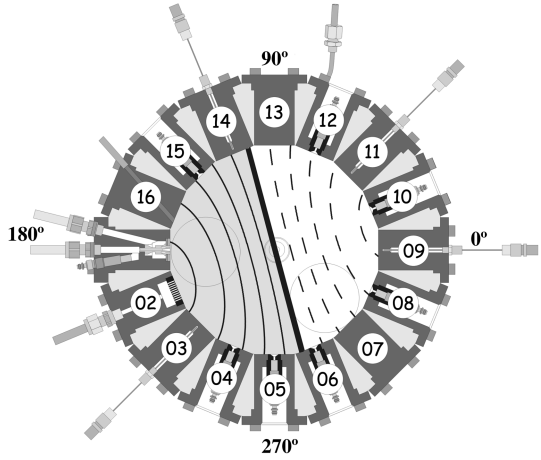

Fig. 19 Nodal line of preferred orientation in the CRC.

mounted in different ports in the cylindrical wall, are forming additional cavities connected to the cylindrical CRC. A modal analysis of the CRC volume taking into account all this additional cavities is shown in Fig. 19 and results in a 1T eigenmode that reproduces the preferred orientation seen in Fig. 18.

Conclusions

It has been shown that the dynamic pressure variation in the CRC in the frequency range of the 1T mode can be well understood by applying the model of a superposition of clockwise and counter-clockwise spinning modes, or from another point of view of a superposition of standing and spinning modes. Using this model the detailed evolution of the acoustic pressure field can be reconstructed with excellent agreement between the experimental data and the model.

The approach enables to get detailed insight in the dynamics of the pressure field. Typical lifetimes of clockwise or counter-clockwise spinning modes can be evaluated, preferred mode orientations can be deduced. The approach thus constitutes a tool for the characterization of acoustic pressure waves in a cylindrical combustor even when the amplitude of the investigated eigenmode is small as compared with the mean pressure fluctuation. The method may help to address the evolution of a HF-instability at an early time when the critical mode still has not gained enough energy from the combustion process to appear as the dominant fluctuating component in the time series of the pressure fluctuation.

References

[1] Harrje, D., and Reardon, F., "Liquid Propellant Rocket Combustion Instability," NASA, SP-194, 1972.

[2] Yang, V., and Anderson, W., editors, *Liquid Rocket Engine Combustion Instability*, Progress in Astronautics and Aeronautics, Vol. 169, AIAA, Washington, D.C., 1995.

[3] Rayleigh, L., "The Explanation of Certain Acoustical Phenomena," *Nature (London)*, Vol. 18, No. 455, 1878, pp. 319–321. doi:10.1038/018319a0
[4] Putnam, A., *Combustion-Driven Oscillations in Industry*, Elsevier, New York, 1971.
[5] Knapp, B., Farago, Z., and Oschwald, M., "Interaction of LOX/GH_2 Spray-Combustion with Acoustics," 45th Aerospace Sciences Meeting, AIAA Paper 2007-0572, Reno, NV, 8–11 Jan. 2007.
[6] Heidmann, M., "Oscillatory Combustion of a Liquid-Oxygen Jet with Gaseous Hydrogen," NASA TN-D-2753, 1965.
[7] Priem, R., "Combustion Stability Specifications and Verification Procedures for Liquid Propellant Rocket Engines," Chemical Propulsion Information Agency Publication 655, 1997.
[8] Clayton, R., Rogero, R., and Sotter, J., "An Experimental Description of Destructive Liquid Rocket Resonant Combustion," *AIAA Journal*, Vol. 6, No. 7, 1968, p. 163.
[9] Litchford, R., and Luo, W., "On Destructive Liquid Rocket Resonant Combustion," 44th AIAA Joint Propulsion Conference, AIAA Paper 2008-5115, Hartford, CT, 2008.
[10] Zucrow, M., and Hoffman, J., *Gas Dynamics*, Vol. 2, 2nd ed., Krieger, Malabar, FL, 1985.
[11] Gröning, S., "Berechnung eines Response Faktors in einer Raketenbrennkammer durch Bestimmung des dynamischen Druckfeldes und einem anschlieÿenden Vergleich mit Flammenemissionsmessungen," Master's Thesis, RWTH Aachen Univ., Aachen, Germany, 2010.
[12] Stearns, S., *Digital Signal Analysis*, Hayden Book Co., Rochelle Park, NJ, 1975.
[13] Conn, A., Gould, N., and Toint, P., *Trust-Region Methods*, Society for Industrial and Applied Mathematics, Philadelphia, PA, 2000.

E. Kim
Associate Editor